Extension of the spectral range of bacteriorhodopsin functional activity by energy transfer from quantum dots

Vladimir Oleinikov[a,b], Nicolas Bouchonville[c], Alyona Sukhanova[a,d], Michael Molinari[c], Svetlana Sizova[a,b], Konstantin Mochalov[a,b], Anton Chistyakov[a,b], Evgeniy Lukashev[a], Aliaksandra Rakovich[e], John F. Donegan[e], Igor Nabiev[a,d,*]

[a] Laboratory of Nano-Bioengineering, Moscow Engineering Physics Institute, 31 Kashirskoe sh., 115409 Moscow, Russian Federation; [b] Shemyakin & Ovchinnikov Institute of Bioorganic Chemistry, Russian Academy of Sciences, 117871 Moscow, Russia; [c] University of Reims Champagne-Ardenne, 51100 Reims, France; [d] Institute of Molecular Medicine, Trinity College Dublin, James's Street, Dublin 8, Ireland; [e] School of Physics, Trinity College Dublin & Centre for Research on Adaptive Nanostructures and Nanodevices, Dublin 2, Ireland

ABSTRACT

Monodispersed semiconductor nanocrystals or quantum dots (QDs) specifically immobilized on the surface of purple membranes (PMs) containing bacteriorhodopsin (bR) can harvest light in the UV to blue region, which cannot be absorbed efficiently by the PMs alone, and transfer the harvested energy to the retinal chromophores of bR via highly efficient Förster resonance energy transfer (FRET). CdTe or CdSe/ZnS QDs with a quantum yield as high as 70% have been used to estimate different parameters characterizing the improvement of the bR biological function caused by nanocrystals. AFM examination has shown that the most FRET-efficient QD–PM hybrid structures are characterized by the highest level of QD ordering; hence, AFM imaging of bR–PM hybrid materials provides the basis for optimization of the assembly design in order to engineer bio-hybrid structures with advanced optical and photovoltaic properties. Oriented bR-containing proteoliposomes tagged with QDs at a QD-to-bR molar ratio of up to 1:5 have been engineered and used to analyze the photoresponse, with the bR proton pumping considerably increased. Finally, the kinetics of the potential/current generation in films of oriented bR containing or not containing QDs have been analyzed. Incorporation of QDs resulted in an increase in the potential/current generation rate and in an almost fourfold increase in the rate of M-form formation. Thus, the improvement of the bR native function by QDs may be caused by two reasons: an extension of the range of utilized light and an increase in the rate of the bR photocycle.

Keywords: bacteriorhodopsin, purple membranes, quantum dots, energy transfer, AFM imaging, hybrid materials

1. INTRODUCTION

Purple membranes (PMs) of the bacteria *Halobacterium salinarum* are unique natural membrane protein crystal patches where a single integral protein bacteriorhodopsin (bR) forms trimers organized into ultrastable lattice with a unit-cell dimension of 6.2 nm. The photochromic and photoelectric properties of bR are related to its biological function[1]. Upon absorption of light, bR undergoes a cyclic sequence of conformational transitions between distinguishable photo-intermediate states accompanied by transport of protons from the cytoplasmic to the extracellular surface of the PM. The high quantum yield of the initial bR state guarantees an efficient photoisomerization of the bR-linked chromophore (retinal) located near the middle of the PM, at a distance of about 2.5 nm from both PM surfaces[2]. The proton transport within the PM consists of the initial charge separation and the de- and re-protonation of retinal[3]. The intra- and extra-cellular surfaces of the PM have different charges, providing a permanent dipole moment facilitating the fabrication of highly oriented PM films[4].

* igor.nabiev@gmail.com

Nanobiosystems: Processing, Characterization, and Applications V, edited by Norihisa Kobayashi, Fahima Ouchen, Ileana Rau, Proc. of SPIE Vol. 8464, 84640Z
 · doi: 10.1117/12.929764

Since the evolution of nature has often solved problems similar to those that humans attempt to solve in harnessing organic compounds, bioelectronics and biophotonics seem to be of considerable promise. Much of the current research effort in this field is related to self-assembled monolayers and protein-based photonic devices[5]. Although a number of proteins have been explored from the point of view of bioelectronic device applications[6,7], bR has received the most attention. A substantial number of publications and patents in this area is a strong indicator that the use of bR in technical applications is a technological reality[8]. One of the domains for effective competition of bR with the existing technologies is dynamic applications where thousands of cycles between two or more distinguishable and reversible states are required[3]. In addition, the photocycle of bR is a complicated process where the molecules undergo a sequence of photodistinguishable conformational transitions. Furthermore, this process may be influenced by additional illumination at wavelengths corresponding to the absorbance bands of some selected photointermediates. In this study, we have demonstrated the effect of quantum dots (QDs) on the bR basic state alone, their action increasing the efficiency of the main biological function of bR, transmembrane pumping of protons. The use of QDs of different, carefully selected colors may specifically affect some selected intermediates of the bR photocycle, thus permitting the development of more complex hybrids with metastable or stable states, paving the way for the development of novel optoelectronic switches or memory elements, respectively.

Therefore, we have investigated the possibility of extension of the spectral range of the bR functional activity by energy transfer from ODs. In other words, photoluminescent QDs served as energy convertors that absorbed light within a wide range of photon energies (the entire solar spectrum) and transferred the harvested energy to the bR chromophore (retinal).

2. MATERIALS AND METHODS

2.1 Materials

Purple membranes (PMs) containing wild-type bacteriorhodopsin (bR) were prepared and purified according to the protocol adapted from Ref. [9]. PMs were dissolved in water to obtain a stock solution with an absorbance of ~0.2 at 568 nm.

Thioglycolic acid (TGA)-stabilized CdTe NCs were synthesized and purified by previously reported methods[10]. CdSe/ZnS QDs have a core of cadmium selenide with a zinc sulphide shell. To make them water-soluble, QDs were treated with DL-cysteine (cys-QD) using the procedures published before[11]. Surface treatment of QDs with low-molecular-weight mercapto-compounds (e.g. with DL-cysteine), instead of the generally accepted encapsulation of QDs in an additional PEG-based shell, yields water-soluble CdSe/ZnS QDs of the smallest possible diameter. QDs solubilized in this way demonstrate a stronger quenching of QD luminescence with bR due to the FRET effect, much exceeding the FRET efficiencies obtained for the hybrid materials made from PEG-encapsulated CdSe/ZnS QDs of larger diameters. All prepared QDs were characterized using dynamic light scattering (DLS) and electrophoresis techniques using a Zetasizer Nano ZS Malvern instrument. The characteristics of QDs used in the study (hydrodynamic and "physical" diameters and zeta-potentials) are shown in Table 1.

Doubly purified deionized water from an 18MΩ Millipore system was used for all dilutions. QDs were diluted with water to obtain clear solutions with an absorbance of ~0.15 at the first excitonic peak. Both bR and QD stock solutions were sonicated for 10 s and 1 min, respectively, prior to measurements. The bR-to-QD ratio was gradually increased by adding small volumes of the PM stock solution to 1 mL of the QD solution. After every addition, absorption, PL, and lifetime measurements were performed. For estimating the pH response of the system, freshly prepared 1 M NaOH was used to raise the pH of the solutions.

Preparation and characterization of hybrid materials. QDs with controlled zeta potential of their surfaces were bound to bR as described here. Both PM and QD stock solutions were sonicated for 10 sec and 1 min, respectively, prior to assembly. The assembling procedure was controlled by analysis of quenching of the QD fluorescence. QDs were always kept at the same concentrations; QD–PM complexes with different molar ratios were obtained by adding different amounts of PMs. In this way, the molar ratios of bR to QDs were discretely varied among samples from 0:1 to 5:1. After addition of PMs, the reaction mixtures were allowed to self-assemble under gentle agitation for 30 min at room temperature.

The QD–PM complexes were further purified by gel filtration on Superdex 200 resin (GE Healthcare) columns equilibrated with 10 mM of sodium ascorbate buffer (pH 6.8). All collected fractions were analyzed by recording their UV–vis spectra, and only those containing QD–PM complexes were used in subsequent experiments. The UV–vis spectra of the complexes were found to be a simple arithmetic sum of the contributions from QDs and bR, which also made it possible to determine the exact bR-to-QD molar ratio for each sample.

The individual samples were diluted with deionized water to a total volume of 2.5 mL and placed into quartz fluorescence cells with an optical path of 10 mm (Hellma, Madrid) for measurements. Control spectra collected from bR in the absence of QD donors were recorded and subtracted from the solution spectra to adjust for parasitic contribution of bR preparations upon direct excitation. To avoid inner filter effects, the QD, PM, and QD–PM preparations with the lowest possible optical densities at the excitation wavelength were used in all experiments. The concentrations used depended on the extinction coefficient of QDs at the excitonic peak, but they were typically within the range 0.5–1.5 μM The assembling procedure was controlled by analysis of quenching of QD fluorescence. The prepared complexes were characterized using AFM. Since the highest FRET efficiencies were obtained for the hybrid materials made from bR and CdTe QDs, these nanocrystals were used in all experiments described below. Cys-solubilized CdSe/ZnS nanocrystals with a controlled surface charge were also prepared and studied in detail to analyze the optimal charge necessary for ensuring the best affinities of QD and PM.

Preparation of proteoliposomes. Proteoliposomes were prepared from soybean lecithin (Sigma, P 5638) containing 14–23% of phosphatidylcholine using the classical protocol of Racker & Stoeckenius[12]. It is known that, in the proteoliposomes prepared according to this protocol, incorporated molecules of bR self-organize into trimers, which, in turn, self-organize into a hexagonal 2D-array similar to that found in native PMs[13,14].

2.2 Experimental methods and data treatment

The absorption spectra were recorded by means of a Varian Cary50Conc UV-visible spectrophotometer. Steady-state photoluminescence measurements were carried out using a Varian CaryEclipse Fluorescence Spectrophotometer (λ_{ex} = 400 nm).

For the AFM measurements, a Nanoscope IIIa (Veeco Instruments, Santa Barbara, CA, USA) equipped with a 10-μm scanner was used. All measurements were made in a liquid environment using a special fluid cell. For isolated PMs, scans were performed in the fluid contact mode using oxide-sharpened PNP-TR tips with a spring constant of 0.32 N/m purchased from Nanoworld. To image the QD–PM material, the experiments were performed in the fluid tapping mode in order to minimize the interactions between the tip and the sample, thus avoiding the possible displacement of the QDs by the tip. The resonance frequency in fluid was around 8 kHz; a PNP-TR tip with a spring constant of 0.08 N/m with a nominal resonance frequency of 17 kHz in air was used for these measurements. For image processing, all raw AFM images were filtered using the fast Fourier transform and wavelet filtering (by convolving Mexican Hat wavelet with the AFM data) by means of the WSxM software.

PL decays were measured using time-correlated single photon counting with the use of a PicoQuant MicroTime 200 instrument. Measurements were performed in ambient conditions, at room temperature, in solutions diluted to obtain reasonable signal intensity. Samples were excited with a picosecond 480-nm laser pulse (PicoQuant LDH-480 laser head controlled by a PDL-800B driver). The overall resolution of the instrument was ~150 ps. The measured PL decays were reconvoluted using nonlinear least-squares analysis. This was done with the SymPhoTime software (PicoQuant) using the equation

$$I(t) \propto \sum_i \alpha_i \exp\left(-t/\tau_i\right) \ , \tag{1}$$

where τ_i are the PL decay lifetimes and α_i are the corresponding pre-exponential factors calculated taking into account the normalization of the initial point in the decay to unity. Weighted residuals and χ^2 values were used to judge on the quality of the fit. A fit with a χ^2 value of less than 1.1 was considered to be good. The τ_i and α_i values obtained from the fit were then used to calculate the average lifetime (τ_{av}) as

$$\tau_{av} = \frac{\sum \alpha_i \tau_i^2}{\sum \alpha_i \tau_i} \ . \tag{2}$$

The energy transfer efficiency (E) was calculated from the average lifetime values as

$$E = 1 - \frac{\tau_{DA}}{\tau_D} \quad , \tag{3}$$

where E is the energy transfer efficiency, and τ_{DA} and τ_D are the average lifetimes of the donors (QDs) in the presence (DA) or absence (D) of the acceptors (bR), respectively.

The expected decrease in the photoluminescence intensity can then be calculated using the following equation:

$$\frac{I_{DA}}{I_D} = 1 - E = \frac{\tau_{DA}}{\tau_D} \quad , \tag{4}$$

where I_{DA} and I_D are the integrated PL intensities of the donors in the presence and absence of the acceptors, respectively.

Measurements of the photoinduced transmembrane proton pumping in a suspension of highly oriented bR-containing liposomes were done through the monitoring of pH variation with a combined glass pH-electrode Accumet (USA) operating in the millivoltmeter mode. Photoexcitation was provided by a home-made source based on a 650 W Osram halogen lamp (Germany) equipped with a 10-cm water filter and a glass IR-cutting filter KG-1 (Schott, USA). The light power density in the optical cell was about 2 kW/m^2. For evaluation of the functional effect of FRET from QDs to bR on the efficiency of proton pumping by bR, 40–70 μL of a 15–25 μM solution of CdTe or CdSe/ZnS QDs (Table 1) were added to the suspension of the proteoliposomes to obtain QD-to-bR molar ratios from 0 to 0.2.

3. RESULTS AND DISCUSSIONS

Monodispersed semiconductor photoluminescent CdTe[10] or CdSe/ZnS[15] QDs have extinction coefficients several orders of magnitude higher than those of organic dyes. QDs are ultrastable against photobleaching, and the quantum confinement effect yields PL emission energy that varies as a function of the size of the QD. The spectral width and position of the optical bands in the QDs can be tailored by controlling their size, and surface chemistry permits adjustment of their surface functionalities.[16-18]

In this study, we have investigated the extension of the spectral range of the bR functional activity by energy transfer from QDs; i.e., we used PL-emitting QDs as energy convertors that absorbed light in a wide range of photon energies (the entire solar spectrum) and transferred the harvested energy to the bR chromophore (retinal). The properties of QDs used in this study are shown in Table 1.

In our experiments, the natural PM purified from the bacteria *Halobacterium salinarum* were bound with CdTe or CdSe/ZnS QDs. In order to develop an efficient hybrid material operating in the FRET regime, we carefully selected the PL colors (diameters) of the QDs (donors of energy) to be optically coupled with the bR retinal chromophore (acceptor), the only chromophore of PMs absorbing light in the visible region, Fig.1.

The retinal linkage with bR (a Shiff base) may be reduced under illumination, and retinal may be further carefully extracted from the PM according to a well-established protocol. This procedure yields so-called white membranes (WMs).19 WMs are excellent control material for studying FRET between QDs and bR. The structure and morphology of the protein and lipid components of WMs are the same as those in PMs, which ensures equal possibilities for eventual nonradiative quenching of QDs after their binding to PMs or WMs, whereas the absence of retinal (the acceptor) completely excludes the FRET channel of QD PL quenching in the QD–WM complex.

We found that the binding of CdTe QDs of different diameters (colors) with PMs led to efficient quenching of exciton emission of QDs, which suggests an efficient FRET from QDs to bR. The assumption that FRET is the main mechanism

of QD quenching mechanism was confirmed by data on comparative quenching of QDs with PMs and WMs. As shown in Fig. 2, the quenching of QDs with WMs was four- to fivefold weaker than that with PMs. This experiment has provided us with the quantitative estimation of the contribution of nonradiative QD quenching and proved that FRET is the main mechanism of QD quenching with PMs.

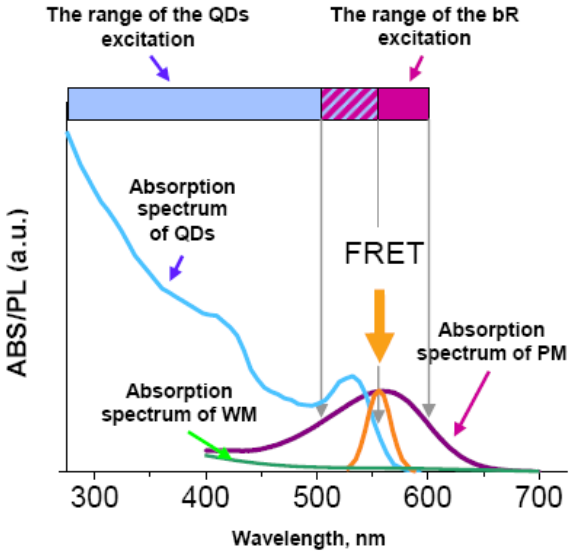

Figure 1. Optical properties of bacteriorhodopsin (bR) in purple and white membranes (PMs and WMs, respectively), and the scheme of energy transfer from quantum dots (QDs) to bR. The UV–vis spectra of PMs (the purple line), WMs (the green line), and one of the types of QDs used in the study (the blue line), as well as the PL emission spectrum of these QDs (the orange line), are shown. The spectral regions of the bR and QD effective excitation are shown as purple and blue bars, respectively.

Table 1. Properties of quantum dots used in the study

Sample*	Maximum of PL emission (nm)	Quantum yield (%)	Diameter (nm)**	Hydrodynamic diameter (nm)***	ζ-potential (mV)
Cys-QD530-CdSe/ZnS	533	40	2.5	5 ± 1	-29.2
Cys-QD570-CdSe/ZnS	570	48	3.1	6 ± 2	-33.4
Cys-QD600-CdSe/ZnS	599	42	4.6	9 ± 2	-37.5
QD550 CdTe	545	34	2.8	4 ± 1	-23.8
QD590 CdTe	589	24	3.3	6 ± 2	-24.8
QD600 CdTe	597	36	3.4	6 ± 1	-25.4
QD650 CdTe	650	29	3.8	7 ± 3	-37.6

* For all measurements, QD concentrations of 0.5–1.5 μM were used. In all cases, the absorbance at the first exciton band was <0.10.

** The diameters of the fluorescing CdTe and CdSe cores.

*** The hydrodynamic diameters have been measured using the dynamic light scattering (DLS) technique. The presented values are averaged over three independent experiments for each QD sample. The errors represent the standard deviations for these three independent experiments with each sample.

We found the difference in the quenching of CdTe QDs of two different colors (diameters) with PMs. The smaller QD590 were quenched more efficiently at the same bR-to-QD molar ratios compared to the quenching of QD650 PL. This difference in quenching behavior is expected when one considers a smaller donor–acceptor distance between the QD and the retinal of bR, as well as a wider spectral overlap between the PL band of CdTe QD590 with the extinction spectrum of the bR ground state.

It should be mentioned that quenching of CdSe/ZnS QD solubilized and stabilized in aqueous solutions with PEG-based polymers or with the low-molecular-weight amino acid Cys was always much weaker than that for CdTe QDs used in the study. We attribute this fact to the larger diameter of CdSe/ZnS QDs compared to CdTe QDs due to the thickness of the additional ZnS shell and an additional organic shell formed during the water solubilization of CdSe/ZnS QDs (Table 1), which reduces FRET.

Together with the steady-state PL studies, time-resolved PL data provided further evidence for FRET within the bR–QD hybrid material. In particular, the average lifetime for a complex consisting of ~0.5 bR molecules per CdTe QD650 was found to be decreased from 10 to 8 ns, which constitutes a decrease of about ~20%. This decrease in the average radiative lifetime of QD PL is expected in the case of FRET, because the energy transfer from QDs to retinal provides an additional kinetic pathway for the decay of QD PL. Note that the integrated PL intensity for this complex was decreased by ~19%; so, there is a very good agreement between the two values. Similar correlations, though for much less efficient PL quenching and lifetime variation, were also observed for CdSe/ZnS–PM complexes (Table 2 and Fig. 3). All these data confirm that FRET is the main mechanism of the quenching of QD PL with PMs.

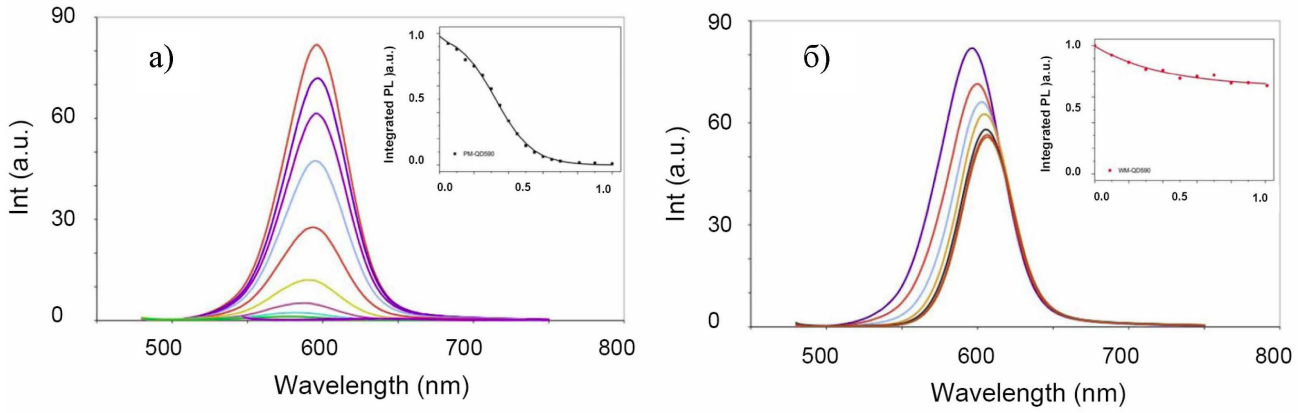

Figure 2. PL intensity as a function of the bacteriorhodopsin to quantum dot (QD) molar ratio. Variation of integrated PL of CdTe QD590 (λ_{em} = 590 nm) as a function of the concentrations of (a) purple membranes or (b) white membranes. The concentration of QDs was fixed at 1.4 μM. The optical densities in these experiments were always about 0.07–0.08.

We have also estimated the increase in the efficiency of the bR biological function in the presence of QDs. We prepared oriented proteoliposomes (Fig.4), i.e., lipid vesicles (liposomes) with bR molecules incorporated in their walls in a highly oriented manner. Proteoliposomes with an average diameter of 57 nm were formed according to the classical protocol of Racker & Stoeckenius.[12] These proteoliposomes have a surface density of 0.06 nm^{-2}, which corresponds to the density of hexagonal bR lattice package in native PMs. In contrast to the bacterial PMs, where bR pumps protons out of the cell, the orientation of bR in the proteoliposomes prepared according to the protocol of Racker & Stoeckenius is known to be opposite, and the protons are pumped into the proteoliposomes.[20] As a result, photoillumination provokes a photoinduced decrease in the concentration of protons (increase in pH) in a suspension of proteoliposomes.

We investigated the photoinduced pH-response of proteoliposomes and found that the photoinduced pH-response detected in the suspension of our proteoliposomes was reversible and the variation of pH at the light illumination intensities used was typical of preparation of extremely highly oriented bR-containing proteolipisomes (Fig. 5). Note that switching off of illumination leads to a complete relaxation of the system to the initial pH value. Our experiments with a hybrid material obtained by immobilization of semiconductor QDs on the surface or in the lipid membrane of proteoliposomes showed that integration of CdTe QD590 in a PM even at QD-to-bR molar ratio of 1:5 induced a pronounced (>25%) increase in the photoresponse in terms of bR proton pumping.

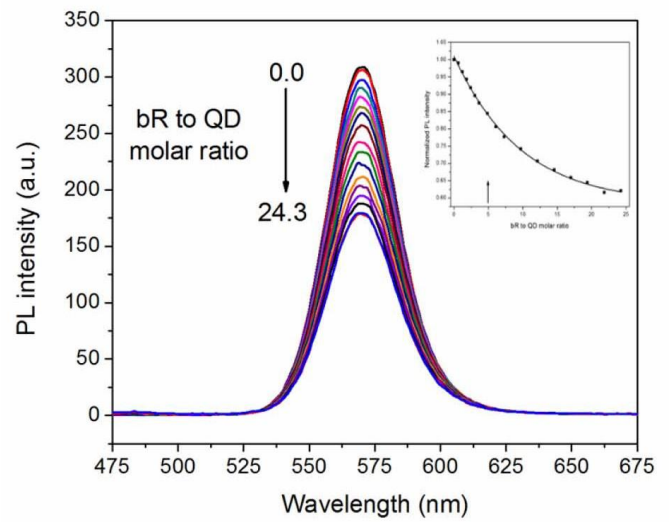

Figure 3. Initial QD concentration was ~0.9 μM. Excitation at 450 nm. The arrow indicates the bRh to QD molar ratio used in photoinduced pH response measurements. A decrease in the QD PL of ~ 17% was observed at this ratio, which agrees with the maximum increase in the proton pumping efficiency of 15% and FRET efficiency of 18% determined from time-resolved PL measurements (Table 2).

It should be emphasized that the thickness of the organic shell coating the QD fluorescent core is essential both for the efficiency of FRET and for the increase in the bR biological function. The efficiency of FRET and the increase in photoresponse were found to be maximum for CdTe QDs covered with TGA forming the stabilizing shell with a thickness of less than 0.3 nm.

The protecting organic shell of CdSe/ZnS nanocrystals (Table 1) is thicker; it is even comparable with the Förster radius of these nanocrystals (R_F = 5.6 nm)[21]; therefore, the efficiency of FRET from these nanocrystals to bR is much less than that for CdTe QDs. Nevertheless, even for CdSe/ZnS QDs, an increase in the efficiency of proton pumping in bR-containing proteoliposomes in the presence of nanocrystals was also detected, although it did not exceed 15%. Moreover, this value agrees with the ~17% decrease in the CdSe/ZnS QD fluorescence for this bR-to-QD ratio (Fig. 3), as well as with the FRET efficiency of ~18% (PL time-resolved data, Table 2).

Table 2. Quenching of CdSe/ZnS QD570 luminescence by bacteriorhodopsin and corresponding changes in radiative lifetime.

bR-to-QD molar ratio	τ (ns) * ± 0.15	E (%) ± 2%	1-E (= τ_{DA}/τ_D) ± 0.02	I_{DA}/I_D **
0.0	4.79	0	1.00	1
2.4	4.35	9.2	0.91	0.919
3.6	4.13	13.8	0.86	0.875
6.1	3.84	19.8	0.80	0.806
12.1	3.7	22.8	0.77	0.707
21.8	3.53	26.3	0.74	0.616

* τ is the average radiative lifetime of a bR–QD complex calculated according to Equation (2). E is the FRET efficiency (Equation 3); (1-E) is the expected PL intensity of the complex when energy transfer is taken into account (Equation 4); I_{DA}/I_D is the PL of the complex obtained from integrated steady-state PL data; ** Error was ~0.002 for bR-to-QD molar ratios of 0.0–5.0 and ~0.001 for higher ones.

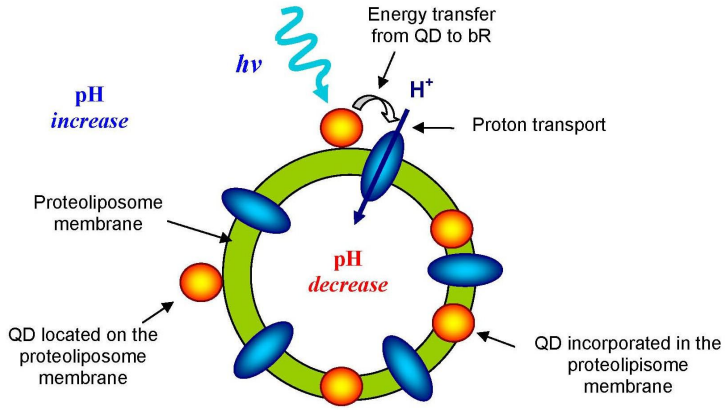

Figure 4. Organization and functionality of a complex composed of liposomes containing highly oriented bacteriorhodopsin (proteoliposomes) and quantum dots (QDs) immobilized on the surface or in the lipid membrane of the proteoliposomes. Photons of higher energy (blue) excite QDs, they fluoresce in the visible region, and the energy from QDs is transferred to bR via FRET. Absorption of photons by bR induces transfer of the proton into the proteoliposome and photoinduced increase in pH in the solution outside of proteoliposomes, which serves as a measure of the efficiency of the bR function.

The photoresponse of bR within the hybrid material increases exponentially with an increase in the photoillumination power density and reaches saturation at about 2 kW/m^2 (Fig. 5). Note that the increase in photoresponse due to the presence of QDs is the maximum at the highest illumination power densities and depends on the amount of QDs incorporated in the proteoliposomes. Binding of QDs in amounts exceeding one QD per bR molecule leads to a decrease in the efficiency of bR proton pumping (Fig. 5). This may be explained by the internal filter effect due to the large quantity of QDs forming multilayers or unbound nanocrystals in the suspension. All these nanocrystals may not participate in FRET with bR, but they block the photoexcitation of bR due to the internal filter effect.

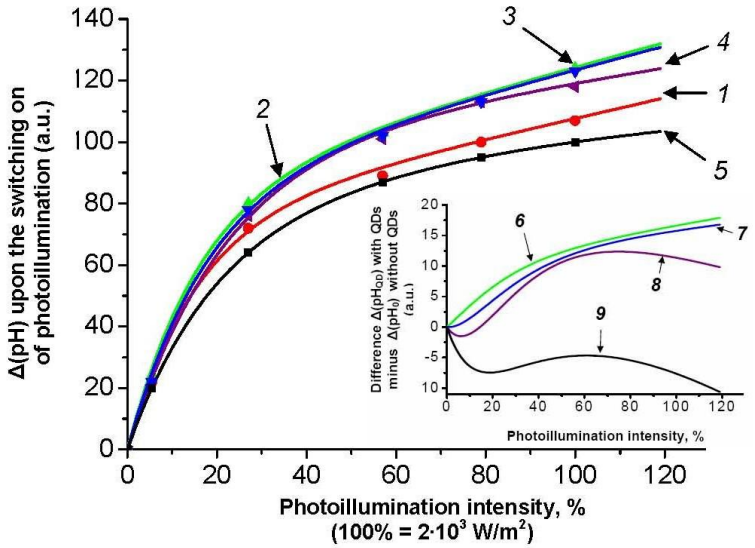

Figure 5. The amplitude of the pH jump Δ(pH) versus the intensity of photoillumination for different contents of CdSe/ZnS quantum dots (QDs; λem = 530 nm) solubilized with PEG–OH. Inset: The difference between Δ(pHQD) and Δ(pH0); here, Δ(pH0) is the jump of pH for the liposome solution without QDs, and Δ(pHQD) is the jump of pH for the proteoliposomes containing QDs. Curve 1, without QDs; curves 2, 3, 4, and 5, after the addition of 5, 10, 15, and 20 µl of a 7.7 mg/ml CdSe/ZnS QDs dispersion, respectively, to the liposome solution; curves 6, 7, 8, and 9 have been obtained by subtracting curve 1 from curves 2, 3, 4, and 5, respectively.

Estimation based on the analysis of the excitation and absorption spectra of bR, as well as the excitation/emission spectra of QDs, yields a maximum increase in the proton transport efficiency of 8–10%. The actual increase in the efficiency is even higher. Moreover, at the highest photoirradiation intensities in the region of saturation, where bR receives enough photons for the highest efficiency of proton transport, addition of QDs has a positive effect (Fig. 5). Such an unexpected behaviors may be explained by the shift of equilibrium between the intermediate states and shortening of the bR photocycle duration. This results in an increase in the number of photocycles per unit time and, consequently, the number of protons transported through the membrane.

This conclusion is confirmed by our measurement of the kinetics of the potential/current generation in films of oriented bR containing or not containing QDs (Fig. 6). Modification of the PM by QDs results in an increase in the potential/current generation rate (Figs. 6A, 6C). These processes are caused by M-intermediate formation, when a proton leaves a Schiff base and passes to the ionized acceptor $D85^{-}$. The rate of M-form formation measured by the flash photolysis method at 410 nm under the conditions of membranes dehydration increases almost fourfold (about 20 μs) in comparison with the water environment (80 μs). In our case (Figs. 6A, 6C), the characteristic time of the reaction is 15–20 μs. What is the most important, proton pumping is accelerated in PMs containing QDs,. Thus, modulation of the native function of bR by QDs may be caused by two reasons: an extension of the range of utilized light and an increase in the rate of the bR photocycle.

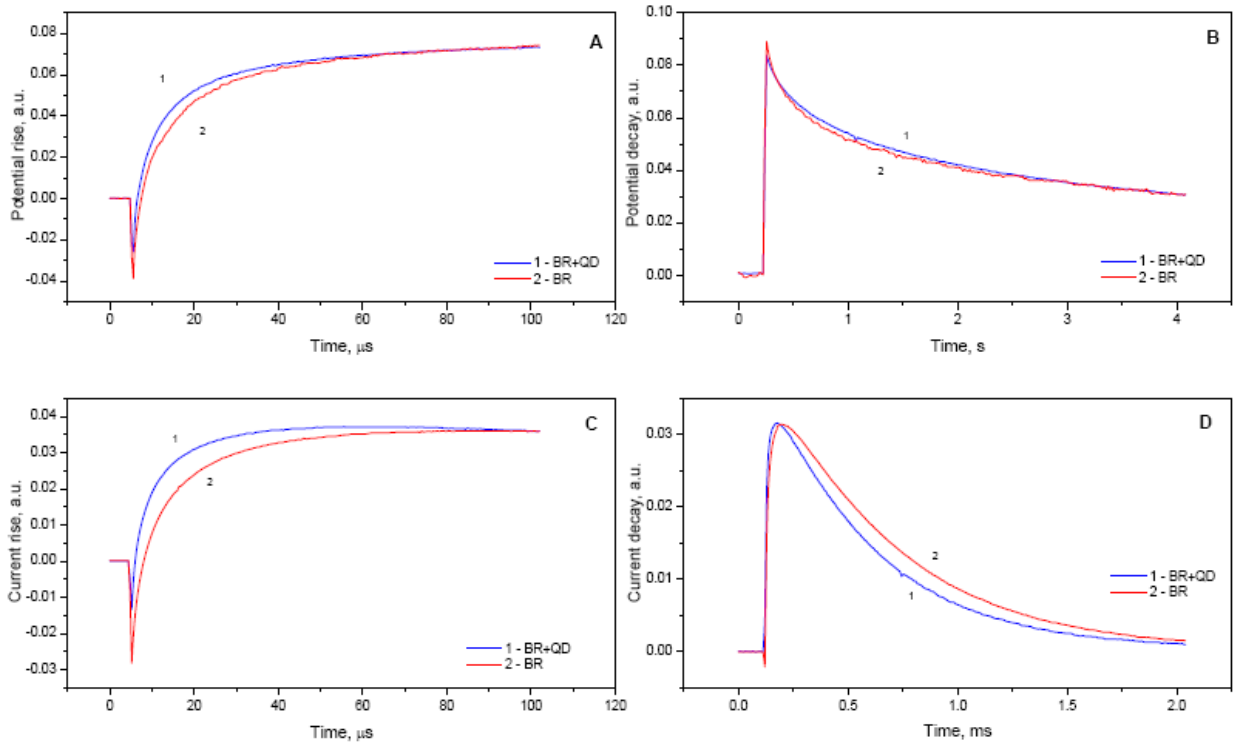

Figure 6. Kinetics of the (A, B) photopotential and (B, C) photocurrent generation in an oriented PM film containing QD570 (curves 1) and not containing quantum dots (curves 2 serving as control).

Note that PMs contain 19 lipid molecules per bR molecule. Therefore, the average surface charge of a PM is negative, because it is determined by the charge of the heads of the lipid PO_3^- groups. A bR molecule itself contains 14 positively charged (basic) lysine and arginine residues. The cytoplasmic surface of a bR molecule contains nine exposed positive groups, and three positive bR groups are exposed on the exterior surface of the PM.[20] This means that the cytoplasmic surface of the PM contains a sufficient number of positively charged groups, which are located exactly at the sites of bR

trimer location. This explains why, at relatively low QD-to-bR ratios, the negatively charged QDs interact specifically with bR trimers on the surface of the PM, rather than with the negatively charged surface of the lipids.

Thus, we have demonstrated that QDs specifically immobilized on the surface a PM can serve as built-in light energy convertors harvesting light that would not have been absorbed efficiently by the PM itself (in the region from UV to blue). Membrane-immobilized QDs have been further demonstrated to be able to transfer the harvested energy via highly efficient FRET to this complex biological system. Finally, we have presented the first proof-of-the-principle evidence that bR as a component of an engineered QD–PM hybrid material can utilize the additional energy transferred by QDs, which improves the efficiency of the bR biological function.

4. ACKNOWLEDGMENTS

This study was supported by the Ministry of Higher Education and Science of the Russian Federation (grants nos. 11.G34.31.0050 and 11.519.11.2005) and by the European Commission through the FP7 Cooperation Program (grant no. NMP-2009-4.0-3-246479 NAMDIATREAM). V.O. acknowledges support of the Russian Foundation for Basic Research (RFBR, grant no. 12-04-00779). The authors thank Vladimir Ushakov for the help in preparation of the manuscript.

REFERENCES

[1] Dale, H., Angevine, C. M. and Krebs, M. P., "Ordered membrane insertion of an archaeal opsin in vivo," Proc. Natl. Acad. Sci. USA, 97, 7847-7852 (2000).

[2] Nabiev, I., Efremov, R. G. and Chumanov, G. D., "The chromophore-binding site of bacteriorhodopsin. Resonance and surface-enhanced resonance Raman spectroscopy and quantum chemical study," J. Biosciences, 8, 363-373 (1985).

[3] Vsevolodov, N. N., [Biomolecular electronics. An introduction via photosensitive proteins], Birkhauser, Boston, 125 (1998).

[4] Oesterhelt, D., "The structure and mechanism of the family of retinal proteins from halophilic archaea," Curr. Opin. Struct. Biol., 8, 489-500 (1998).

[5] Birge, R.R., Gillespie, N.B., Izaguirre, E.W., Kusnetzow, A., Lawrence, A.F., Singh, D., Song, Q.W., Schmidt, E., Stuart, J.A., Seetharaman, S., Wise, K.J., "Biomolecular electronics: Protein based associative processors and volumetric memories," J. Phys. Chem. B, 103, 10746-10766 (1999).

[6] Boxer, S. G., Stocker, j., Franzen, S. and Salafsky J., [Re-engineering photosynthetic reaction centers. In Molecular Electronics-Science and Technology" (ed. Aviram, A.)], American Institute of Physics, New York, 262, 226-241 (1992).

[7] Lee, I., Lee, J. W. and Greenbaum, E., "Biomolecular electronics: vectorial arrays of photosynthetic reaction centers," Phys. Rev. Lett., 79, 3294-3297 (1997).

[8] Rakovich, A., Sukhanova, A., Bouchonville, N., Lukashev, E., Oleinikov, V., Artemyev, M., Lesnyak, V.., Gaponik, N., Molinari, M., Troyon, M., Rakovich, Yu., Donegan, J.and Nabiev, I., "Resonance energy transfer improves the biological function of bacteriorhodopsin within a hybrid material built from purple membranes and semiconductor quantum dots," Nano Lett., 10, 2640–2648 (2010).

[9] Oesterhelt, D. and Stoeckenius, W., "Isolation of the cell membrane of Halobacterium halobium and its fractionation into red and purple membrane," Methods Enzymol., 31, 667-678 (1974).

[10] Rogach, A. L.; Franzl, T., Klar, T.A., Feldmann, J., Gaponik, N., Lesnyak, V., Shavel, A., Eychmller, A., Rakovich, Y. P., Doneganet, J.F., "Aqueous synthesis of thiol-capped CdTe nanocrystals: State-of-the-art," J. Phys. Chem. C, 111, 14628–14637 (2007).

[11] Williams, Y., Sukhanova, A., Nowostawska, M., Davies, A.M., Mitchel, S., Oleinikov, V., Gun'ko, Y., Nabiev, I., Kelleher, D., Volkov, Y., " Probing cell type-specific intracellular nanoscale barriers using size-tuned quantum dots," Small, 5, 2581-2588 (2009).

[12] Racker, E. and Stoeckenius W., "Reconstitution of purple membrane vesicles catalyzing light-driven proton uptake and adenosine triptosphate formation," J. Biol. Chem., 249, 662-663 (1974).

[13] Sternberg, B., L'Hostis, C., Whiteway, C. A. and Watts, A., "The essential role of specific Halobacterium halobium polar lipids in 2D-array formation of bacteriorhodopsin," Biochim. Biophys. Acta, 1108, 21-30 (1992).

[14] Shibakami, M., Tsuihiji, H., Miyoshi, S., Nakamura, M., Goto, R., Mitaku, S., Sonoyama, M., "Reconstitution of bacteriorhodopsin into cyclic lipid vesicles," Biosci. Biotechnol. Biochem., 72, 1623-1625 (2008).

[15] Murray, C. B., Kagan, C. R. and Bawendi, M. G., "Synthesis and characterization of monodisperse nanocrystals and close-packed nanocrystal assemblies", Annu. Rev. Mater., 30, 545-610 (2000).

[16] Resch-Genger, U., Grabolle, M., Cavaliere-Jaricot, S., Nitschke, R. and Nann, T., "Quantum dots versus organic dyes as fluorescent labels," Nature Meth., 5, 763-775 (2008).

[17] Nabiev, I., Sukhanova, A., Artemyev, M. and Oleinikov, V., [Fluorescent colloidal particles as a detection tools in biotechnology systems", In Colloidal Nanoparticles in Biotechnology (ed. Elaissari, A.)], Wiley & Sons Inc., Ch. 6, 133-168 (2008).

[18] Howarth, M., Liu, W., Puthenveetil, S., Zheng, Y., Marshall, L.F., Schmidt, M.M., Wittrup, K.D., Bawendi, M.G., Ting, A.Y., "Monovalent, reduced-size quantum dots for imaging receptors on living cells," Nature Meth.,. 5, 397-399 (2008).

[19] Birnbaum, D. and Seltzer, S., "A highly reactive heteroatom analog of retinal and its interaction with bacteriorhodopsin," Photochem. Photobiol., 55, 745-752 (1992).

[20] Oesterhelt, D. and Stoeckenius, W., "Functions of a new photoreceptor membrane," Proc. Natl. Acad. Sci. USA, 70, 2853-2857 (1973).

[21] Sukhanova, A., Susha, A.S., Bek, A., Mayilo, S., Rogach, A.L., Feldmann, J., Oleinikov, V., Reveil, B., Donvito, B., Cohen, J.H., Nabiev, I., "Nanocrystal-encoded fluorescent microbeads for proteomics: antibody profiling and diagnostics of autoimmune diseases," Nanoletters, 7, 2322-2327 (2007).